Virus–antibody interactions

DOI: 10.1002/smll.200600006

Submicrometer Pore-Based Characterization and Quantification of Antibody–Virus Interactions**

*Jeffrey D. Uram, Kevin Ke, Alan J. Hunt, and Michael Mayer**

This paper describes the use of a submicrometer pore-based resistive-pulse sensor to 1) detect a specific virus or a virus-specific antibody in solution, 2) probe the ability of an antibody to immunoprecipitate the virus, 3) determine the number of antibodies bound to individual virus particles, and 4) monitor the assembly of nanoparticles onto templates (here antibodies onto viruses) in situ. The assay is label-free, examines viruses in their native, assembled state, and requires no immobilization or modification of the virus or antibody. It functions by detecting the difference in the peak amplitudes of resistive pulses that occur when viruses with and without antibody bound pass through a submicrometer pore. This technique made it possible to monitor quantitatively the time-course of the binding of an antibody to a nonpathogenic virus, the icosahedrical *Paramecium bursaria* chlorella virus (PBCV-1) with a diameter of ≈ 190 nm.[1] We found that the maximum number of antibodies that were able to bind to PBCV-1 was 4200 ± 450. Due to its small footprint and its simple detection scheme, submicrometer pore-based sensing of antibody–virus interactions may enable portable or high-throughput immunoassays for diagnostics and biodefense.

The ability to determine the number of antibodies bound to a virus enables at least three important applications. First, it makes it possible to predict the efficacy of antibody-mediated neutralization of viruses.[2,3] Second, the number of antibodies that are bound to a virus can be used for determining the antibody's affinity[4,5] and the valency of binding.[6,7] And third, antibodies binding to a virus particle represent an accessible example of a well-defined self-assembly; monitoring this assembly process may thus be useful as a model system for studying templated self-assembly. Such a system may promote other attempts of controlled nanoassemblies (e.g., fabrication of hierarchical nanostructures through the binding of nanoparticles to engineered templates – we are currently investigating this application).[8–12]

Currently available techniques for direct determination of the number of antibodies bound to virus particles include assays with radiolabeled antibodies,[13–18] sodium dodecyl sulfate–polyacrylamide gel electrophoresis (SDS-PAGE),[19] capillary electrophoresis (CE),[20] and enzyme-linked immunosorbent assays (ELISA).[21] These techniques typically require: 1) a minimum concentration of 3×10^9 particles mL^{-1} (ELISA and CE typically use $> 3 \times 10^{11}$ particles mL^{-1}), 2) labeled antibodies, 3) reaction volumes ranging from 10 μL (CE) to ≥ 100 μL, and 4) in most cases, fairly bulky and sophisticated laboratory equipment with high power requirements (such as a CE apparatus, plate readers, etc).

Here we present a simple, nondestructive method for detecting virus-specific antibodies in solution and for determining the number of antibodies bound to an intact virus in a physiological buffer. This label-free technique is able to operate with virus concentrations as low as 5×10^7 particles mL^{-1} and establishes whether or not the antibody can aggregate (immunoprecipitate) the virus. As illustrated in Figure 1, the approach uses laser-fabricated pores in glass and simply measures transient changes in current (so-called "resistive pulses"), which are typical for Coulter-counting experiments. In these experiments, the reaction volume was 40 μL, but this value could be reduced to < 10 μL via the integration of microfluidics.[22] Due to the small size of the pores, this approach could potentially be miniaturized and performed in parallel for high-throughput applications.

Previous work using submicrometer pores, nanopores, and nanotubes for resistive-pulse sensing includes the detection of colloid aggregation,[23,24] DNA,[25–40] nanoparticles,[41–47] proteins,[48–52] small molecules,[53–55] the measurement of the size and polydispersity of several viruses,[56,57] as well as the analysis of the length of viral glycoproteins (spikes).[58] Sohn's group used resistive-pulse sensing to detect the binding of antibodies to synthetic colloids, which were functionalized with antigen.[48,52] Here we demonstrate the use of resistive-pulse sensing for the detection, characterization, and quantification of the binding of antibodies to intact virus particles.

In order to measure the resistive pulses caused by the passage of virus particles through the pore, we used a similar setup to the one reported recently.[51] It consisted of a patch-clamp amplifier with two Ag/AgCl electrodes and a conical pore with a diameter of 650 nm mounted in a poly(dimethylsiloxane) (PDMS) fluidic setup (see Supporting Information for a schematic of the setup and SEM images

[*] Prof. M. Mayer
Departments of Biomedical Engineering and Chemical Engineering
University of Michigan, Engineering Research Building (ERB)
Room 4107, 2200 Bonisteel Blvd.
Ann Arbor, MI 48109-2099 (USA)
Fax: (+1) 734-763-4371
E-mail: mimayer@umich.edu
J. D. Uram, K. Ke
Department of Biomedical Engineering
University of Michigan, Ann Arbor, MI 48109-2099 (USA)
Prof. A. J. Hunt
Department of Biomedical Engineering and Center for Ultrafast Optical Science
University of Michigan, Ann Arbor, MI 48109-2099 (USA)

[**] This work was supported by an NSF career award (M.M.) and by a research grant from IMRA America and AISIN USA as well as seed funds from the College of Engineering, University of Michigan. The authors thank Daniel J. Estes, James Gurnon, and James L. Van Etten for valuable discussions.

Supporting information for this article is available on the WWW under http://www.small-journal.com or from the author.

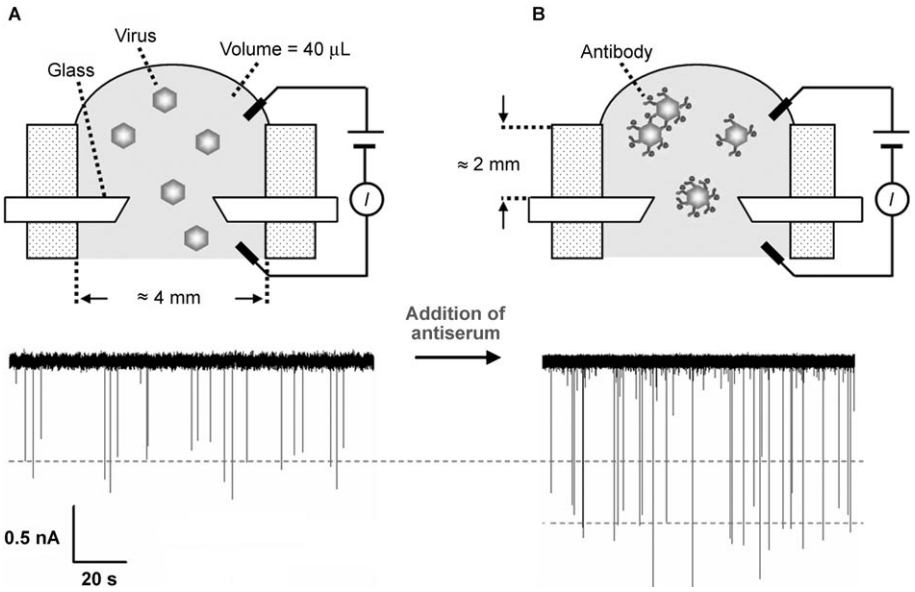

Figure 1. Resistive-pulse technique for detecting and characterizing the binding of antibodies to virus particles. A) Detection of virus particles before addition of antibodies: Single virions passing through the laser-fabricated conical pore cause a transient reduction in current (resistive pulse) as shown by the spikes (events) in the current trace. The dotted line represents the mean of a Gaussian curve fit to the distribution of the peak amplitudes of the events. The concentration of the virus was 4×10^7 particles mL^{-1} and the average current passing through the pore for all experiments was $\approx$140 nA. B) Detection of virus particles after addition of antibodies: Binding of antibodies to the virus increases the volume of the particle leading to an increase in the peak amplitude when the viruses pass through the pore. The current trace displays events that were recorded 10–15 min after addition of the antiserum, which was at a final dilution of 0.001× the original antiserum. If the antibody is capable of causing aggregation of viruses, this approach makes it possible to identify dimers (and larger complexes of virus particles) by detecting events with approximately twice (three times, etc.) the peak amplitude of individual viruses.

of the pores). The pore was fabricated in a borosilicate cover glass using a femtosecond-pulsed laser.[22,51,59–62] We chose glass as the substrate because it is an excellent material for low-noise electrical recordings (i.e., low capacitance, low dielectric loss),[51,63–65] and the conical shape of the pore provided enhanced sensitivity compared to cylindrical pores.[50,51] Replacement of the solutions on either side of the pore was straightforward due to the fluidic setup and the transparency of the entire assembly made it possible to observe the pore with a microscope when necessary.

Before examining the interaction of antibodies with virus particles, we characterized the response of the submicrometer pore to spherical nanoparticles of defined size and shape (see Supporting Information).[51] Deblois et al. demonstrated that a spherical particle passing through a *cylindrical* nanopore creates a resistive pulse with a peak amplitude that was proportional to the volume of the particle (as long as the particle diameter was less than $\approx$40% of the diameter of the pore).[41] We demonstrated recently a linear relationship for spherical particles passing through *conical* pores;[51] the proportionality between current peak amplitude and particle volume for the conical pore was 3.9×10^{-4} pA nm^{-3}. Virus particles are typically not perfectly spherical; however, experimental evidence suggests that the shape of particles that resemble spheroids does not influence the linear relationship between particle volume and peak amplitude.[66] We made use of this linear correlation to estimate the change in the volume of PBCV-1 virus particles before and after antibody binding (Figure 1).

At the beginning of each experiment, we characterized the response of the submicrometer-pore-based Coulter counter to single virions (see Supporting Information for a detailed analysis of the bandwidth of the measurement, the bandwidth and sampling frequency required to resolve an event due to a virus completely, and the effects of digital filtering and decimation of data on the peak amplitudes and half-widths of the events). Even in the absence of antibodies, PBCV-1 virions passing through the conical pore created resistive pulses with peak amplitudes significantly above the baseline noise (Figures 1 and 2). We analyzed these pulses with a computer algorithm by using a threshold value for the peak amplitude to identify individual "virus events" (the dotted red line in Figure 2A and B indicates the threshold value); peaks that had at least 10 times the amplitude of the standard deviation of the current noise from its mean baseline value (root mean square current noise, here called RMS noise) were counted as viruses (most events generated from a solution containing only virus had peak amplitudes of at least 700 pA, or $\approx$40× the RMS current noise). The analysis of resistive pulses showed that the frequency of events was proportional to the concentration of the virus[43,47,56] in a concentration range from 4.4×10^7–2.5×10^9 particles mL^{-1}; we found the following relationship: frequency of events [Hz] $=4.0\times10^{-9}$ [Hz mL particles^{-1}] × concentration of virus particles [particles mL^{-1}]; $N=6$; $R^2=0.95$ (see Supporting Information).

In order to estimate the size of individual virus particles without any bound antibody, we analyzed approximately 1400 virus events (see Supporting Information). This analysis was based on fitting a Gaussian distribution to a histogram of the peak amplitudes as shown in Figure 2C. Applying the linear relationship between peak amplitude and particle volume to the mean peak amplitude from the Gaussian distribution then made it possible to calculate the mean volume of the virus particles. Using equations that relate the volume of an icosahedron to its diameter,[67] we obtained a diameter of 203 ± 14 nm along the fivefold axes for PBCV-1 virions (see Supporting Information for a more detailed discussion). This result compares well with measurements of the size of PBCV-1 by cryoelectron microscopy,

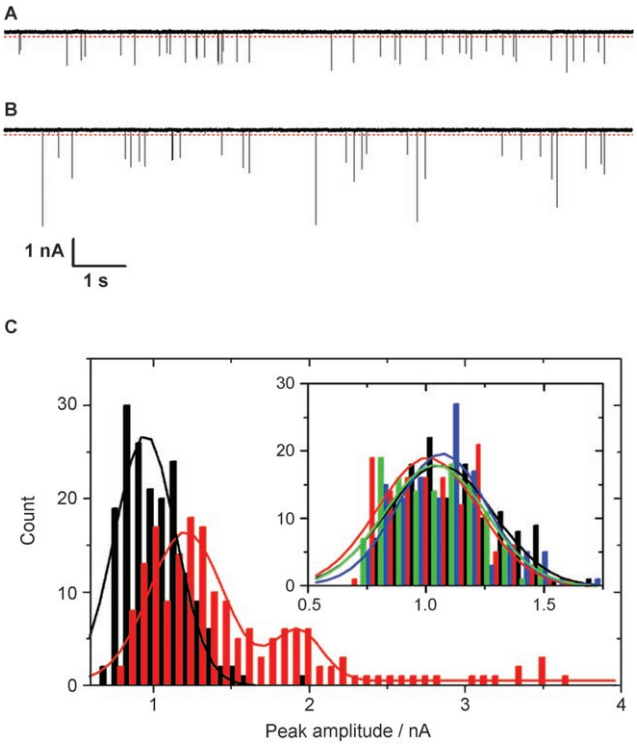

Figure 2. Detection of an antibody–virus interaction using a submicrometer pore. A) Current versus time trace before addition of antiserum: The transient increases in resistance (events) that occurred when viruses passed through the pore led to transient reductions in current. The dotted red line represents the threshold used to distinguish events caused by the passage of viruses from current noise. B) Current versus time trace approximately 8 min after addition of antiserum: The mean peak amplitude was approximately 22% larger than the mean peak amplitude before addition of antiserum, whereas the four largest peaks were presumably due to aggregates of virus particles. C) Histograms of the peak amplitudes of 175 events that occurred before antibody binding (black) and 6–8 min (red) after addition of antiserum (final virus concentration 4.4×10^8 particles mL^{-1}, final dilution of the antiserum: 0.001× the original antiserum). The Gaussian mean of the first (bigger) peak in the red histogram shifted compared to the histogram before antibody binding (shown in black). The second peak in the red histogram occurred presumably due to the formation of dimers. The inset represents data from control experiments; the histograms show events that occurred before (black) and 2.5–3.5 min (red), 7.5–8.5 min (blue), and 13–15 min (green) after addition of serum from a rabbit that was not immunized (final virus concentration 4.4×10^8 particles mL^{-1}, final dilution of this control serum: 0.0013× the original control serum). The change in the mean peak amplitude of the control experiments was $<6.5\%$.

which revealed an average diameter of 190 nm along the fivefold axes (depending on the microscope technique, diameters of 140–190 nm have been reported;[1] however, cryo-electron microscopy is known to preserve the native state of the virus[68,69] and may therefore reflect the size of the virus particles in their hydrated state more accurately than EM techniques that require drying of the samples). Coulter counting with a submicrometer pore is thus a rapid, simple, and effective technique to determine the size of virus particles in their native state.[56,57]

To examine the binding of antibodies to PBCV-1, we monitored the peak amplitude of the events after adding a polyclonal antiserum against PBCV-1; the dilution of the antiserum and therefore the concentration of antibodies in the mixture was kept constant in all experiments while the concentration of virus particles was varied (the concentration of the specific antibody in the antiserum was unknown; however, in the Supporting Information we calculated a lower boundary of 0.55 mg mL^{-1} for the concentration of the specific antibody based on the collected data). Upon addition of antiserum to solutions with various virus concentrations, the peak amplitudes of the virus events increased. A Gaussian fit of the resulting histograms showed a shift of the mean peak amplitude that indicated particles of increased volume (Figure 2C). The final increase in amplitude upon antibody binding onto individual virus particles ranged from +7 to +60% (Figure 3), depending on the ratio of antibody concentration to virus concentration in the solution. By calculating the difference between the mean current peak amplitudes from the Gaussian fits before and after addition of antiserum (Figure 2C), we were able to determine the increase in volume due to antibody binding. The maximum increase in volume occurred at the highest antibody to virus ratio and was $+1.4\times10^6$ nm^3, corresponding to +60% (Figure 1).

Figure 2C also shows a second peak in the histogram of the peak amplitudes upon addition of antibody to the virus particles. The mean value of the Gaussian distribution fitted to the second peak was approximately twice that of the first peak. Since the antiserum that was used can cause aggregation of viruses[70] (see also Supporting Information), we suggest that the second peak was caused by dimers of viruses that were linked by the divalent polyclonal IgG antibodies in the antiserum. Control experiments with serum from a rabbit that was not immunized caused only a small ($<6.5\%$) change of the mean of a Gaussian fit to the peak amplitudes of the virus (Figure 2C, inset), indicating that binding of nonspecific antibodies (or other proteins) to the viruses was minimal.

Using the aforementioned approach to calculate the increase in volume of virus particles upon binding of antibodies, we were able to estimate the number of antibodies attached to individual virus particles by assuming that each antibody contributed a volume of 347 nm^3 (this molecular volume of IgG antibodies was measured by atomic force microscopy).[71] Since the assay presented here provided the ability to record virus events continuously, it was possible to follow the number of antibodies bound to virus particles over time. It was thus possible to extract the kinetics of the antibody–virus interaction at different ratios of antibody concentration to virus concentration as shown in Figure 3A. The equilibrium stage of antibody binding was typically reached after 6–13 min (depending on the ratio of antibody to virus). We found that the equilibrium occupancy decreased with decreasing antibody-to-virus ratio and that it ranged from 500–4000 antibodies per virus particle (Figure 3B).

Based on the sigmoidal fit of the data shown in Figure 3B, we estimate that the maximum number of antibod-

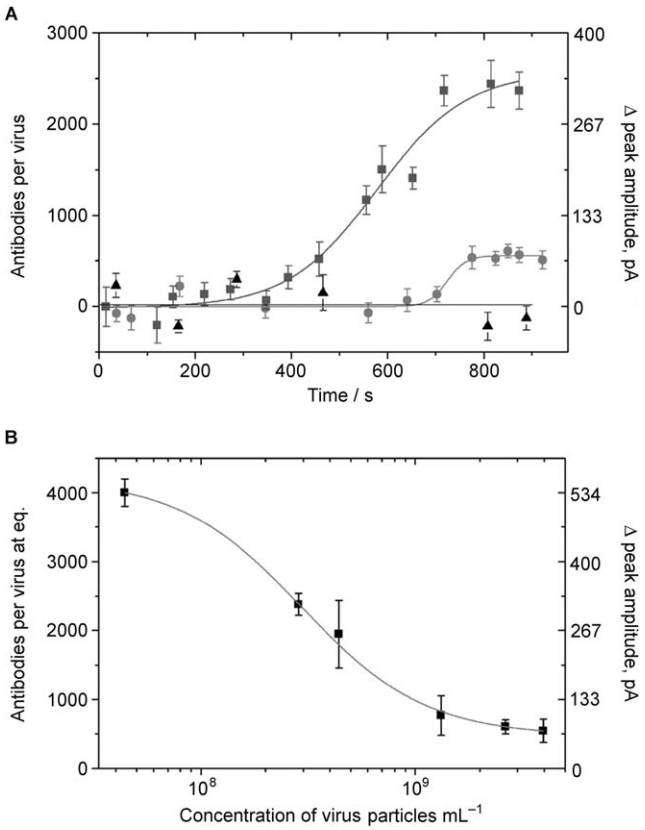

Figure 3. Kinetics of antibody binding at different ratios of antibody to virus concentration and estimation of the maximum number of antibodies that can bind to the virus. In all experiments, the final dilution of the antiserum or control serum was held constant at 0.001 × the original serum. A) Plot of the number of antibodies bound to virus particles versus time. The final concentration of the virus was either 2.8×10^8 (squares) or 4.0×10^9 particles mL^{-1} (circles). The triangles represent a control experiment with nonspecific rabbit serum and a virus concentration of 3.4×10^8 particles mL^{-1}. The error bars reflect the error of the mean value from a Gaussian fit to a histogram of the peak amplitudes of at least 50 events. B) Plot of the number of antibodies bound to PBCV-1 viruses at equilibrium versus the concentration of the virus (increasing virus concentration corresponds to decreasing antibody-to-virus ratio). The data were fitted with a sigmoidal function of the form $y = A2 + (A1 \times A2)/p\,(1+x/x_0)$; $N = 6$, $R^2 = 0.99$. The error bars were calculated by summing the standard deviation of the mean values of the Gaussian fits to histograms of the peak amplitudes.

ies that could bind to the virus particles was 4200 ± 450. Wang et al. report[70] that PBCV-1 contains a major capsid protein which carries the primary epitope to which the polyclonal antiserum binds. PBCV-1 is enclosed in 5040 copies of this major capsid protein.[72] Since we observed a maximum number that was close to this number, namely 4200 ± 450 antibodies bound to each virus particle, we propose that most of these primary epitopes were accessible for antibody binding. The close agreement of these numbers also suggests that the majority of the antibodies in the antiserum were bound to an individual virus particle via one of their two binding sites (i.e., monovalent binding; purely divalent binding would result in a maximum possible antibody load of ≈ 2520 per virus assuming that the major surface antigen is responsible for most antibody-binding interactions). The observation that this antiserum aggregates the virus also supports the hypothesis of significant monovalent binding.

In conclusion, we have developed a simple technique for determining the number of antibodies bound to viruses in their native conformation. The assay is label-free, nondestructive, requires no immobilization or modification of the virus or antibody, and can establish if the antibody is suitable for immunoprecipitation. Due to the specificity of most antibody–virus interactions, this method can be used to detect the presence of an antibody directed against a particular virus in complex media such as serum (here the anti-PBCV-1 antibody); it may therefore be useful for immunoassays[73] and vaccine development. One potential drawback of this technique is that it may be challenging to detect a small number of antibodies (<10) bound to a virus particle. While we applied this method to sense the binding of antibodies to viruses, we expect that this technology could be extended to characterize and monitor other types of nanoscale assemblies such as the assembly of nanoparticles to functional components.[8–12]

Experimental Section

Solutions: All solutions were prepared with deionized water (resistivity of 18.2 MΩ cm, Aqua Solutions, Jasper, GA) and we used potassium chloride, sulfuric acid (both from EMD Biosciences, La Jolla, CA), tris(hydroxymethyl)aminomethane (TRIS; Shelton Scientific, Shelton, CT), bovine serum albumin (Sigma, St. Louis, MO), Tween 20 (Mallinckrodt Chemicals, Phillipsburg, NJ), hydrochloric acid (VWR International, West Chester, PA), nitric acid (Fluka Chemie, Buchs, Switzerland), and hydrogen peroxide (EMD Chemicals, Gibbstown, NJ) without further purification. Recording buffer, composed of 150 mM KCl, 50 mM TRIS buffer, pH 7.8, 0.1 mg mL^{-1} bovine serum albumin, 0.1% w/v Tween 20, was filtered through sterile, low-protein-absorption polyethersulfone membrane filters with a pore size of 0.2 μm (Pall, East Hills, NY). Concentrated PBCV-1 virions and the polyclonal antiserum from rabbit were both kindly provided by J. L. Van Etten (University of Nebraska-Lincoln). We diluted the virus and antiserum in recording buffer and filtered the antiserum solution through a 0.2-μm membrane filter.

Nanomachining using a femtosecond pulsed laser: This procedure was described in detail previously.[51] Briefly, a borosilicate glass cover slide (Corning 0211, Fisher Scientific, Pittsburgh, PA) was attached to a three-axes microscope nanomanipulation stage (Mad City Labs, Inc., Madison, WI); a droplet of water was placed on the area that was to be machined. For laser-based ablation of the glass at defined locations, we focused a directly diode-pumped Nd:glass CPA laser system (Intralase Corp., Irvine, CA) through a 100× oil immersion microscope objective (N.A. = 1.3, Zeiss, Thornwood, NY), and used laser pulses that were frequency doubled from 1053 nm to 527 nm with a duration of 600–800 fs. We used a three-stage process that employed different pulse energy and repetition rates for the shaft, top of the cone, and tip of the cone to machine the pore.

Preparation of the substrates with the pore for SEM: The glass cover slide with the pore was coated in gold (thickness

≈10 nm) using a sputter coater (Structure Probe Incorporated, West Chester, PA) and imaged with a high-resolution scanning electron microscope (FEI Company NOVA 200 Nanolab, Hillsboro, OR).[51] After imaging, the gold layer was removed using a 3:1 mixture of fuming nitric acid and concentrated hydrochloric acid (aqua regia).

Mixing and data analysis: The diluted virus solution was added to the buffer in the top liquid compartment (final volume of this mixture was 40 μL). To keep the concentration of the polyclonal antibodies constant, 2 μL of the diluted antiserum was always added to this virus/buffer mixture. The volume in the top liquid compartment was then aspirated and expelled three times using a pipette (Eppendorf Reference, Westbury, NY) with a volume setting of 5 μL. This procedure combined with the small volume ensured that the two solutions were well mixed.

The addition of the virus to the top liquid compartment caused the RMS noise (filter cutoff frequency = 10 kHz) to change by a maximum of 15.5% (15.6–18.0 pA RMS at a virus concentration of 4.4×10^8 particles mL^{-1}). This change was, however, not correlated with the concentration of the virus; the maximum concentration of virus (4×10^9 particles mL^{-1}) caused a change of only 3%. Addition of the antiserum to the top liquid compartment caused the RMS noise to change by less than 4%.

During the data analysis, we usually noticed that immediately after the addition of antiserum or control serum the peak amplitude from virus particles of the events was slightly reduced (<4.7%). This decrease in amplitude was attributed to a small change in the conductance of the solution. In order to minimize the error in our determination of the number of antibodies bound to a virus, we used the average of the Gaussian means of the peak amplitudes, measured immediately after addition of antiserum (before significant binding of antibodies could occur) as the peak amplitude of virus particles that did not have antibodies bound on their surface.

Data acquisition and processing: Prior to each experiment, the glass cover slide that contained the pore was cleaned in a fresh mixture of 3:1 concentrated sulfuric acid to 30% hydrogen peroxide for at least 15 min. The poly(dimethylsiloxane) (PDMS, Sylgard 184 Silicone, Dow Corning, Midland, MI) support that contained the bottom liquid compartment (see Supporting Information) was cleaned thoroughly after each experiment with alternating rinses of deionized water and 95% ethanol (VWR International). We cut the PDMS film that was used for the top liquid compartment from a slab of PDMS that was cured in a clean Petri dish; a new PDMS film was used in each experiment. This procedure ensured a good seal between the PDMS and the glass, and no leaks were encountered during the experiments. Ag/AgCl pellet electrodes (Eastern Scientific, Rockville, MD) were used since the recorded currents were relatively large (≈140 nA). A patch-clamp amplifier (Axopatch 200B) was used in voltage clamp mode and the analog low-pass filter was set to a cutoff frequency of 100 kHz. The setup was completed by a low-noise digitizer (Digidata 1322, sampling frequency set to 500 kHz), and a computer with recording software (Clampex 9.2) for data acquisition. For all data processing and event collection, Clampfit 9.2 (all from Axon Instruments, Union City, CA) was used.

Data was filtered with a digital Gaussian low-pass filter with a cutoff frequency of 10 kHz and then decimated to a sampling frequency of 50 kHz (see Supporting Information for a detailed analysis of the bandwidth of the measurement, the bandwidth and sampling frequency required to resolve an event due to a virus completely, and the effects of digital filtering and decimation of data on the peak amplitudes and half-widths of the events). We defined a peak as an "event" that was due to passage of a virus if the signal had an amplitude of at least 13 times the standard deviation of the baseline signal from its mean for a duration of at least 25 μs and a maximum of 10 ms (all events had a halfwidth >100 μs). The collected data was analyzed using Origin 7.5 (OriginLab, Northampton, MA) and Matlab (The MathWorks, Natick, MA).

Keywords:

antibodies · immunoassays · self-assembly · sensors · viruses

[1] J. L. Van Etten, R. H. Meints, *Annu. Rev. Microbiol.* **1999**, *53*, 447–494.
[2] P. W. H. I. Parren, D. R. Burton, *Adv. Immunol.* **2001**, *77*, 195–262.
[3] P. J. Klasse, Q. J. Sattentau, *J. Gen. Virol.* **2002**, *83*, 2091–2108.
[4] M. H. V. Van Regenmortel, *Mol. Immunol.* **1988**, *25*, 565–567.
[5] J. L. Pellequer, M. H. V. Van Regenmortel, *Mol. Immunol.* **1993**, *30*, 955–958.
[6] N. J. Dimmock, S. A. Hardy, *Rev. Med. Virol.* **2004**, *14*, 123–135.
[7] Z. Che, N. H. Olson, D. Leippe, W. Lee, A. G. Mosser, R. R. Rueckert, T. S. Baker, T. J. Smith, *J. Virol.* **1998**, *72*, 4610–4622.
[8] C. M. Niemeyer, *Angew. Chem.* **2001**, *113*, 4254–4287; *Angew. Chem. Int. Ed.* **2001**, *40*, 4128–4158.
[9] P. Hazarika, B. Ceyhan, C. M. Niemeyer, *Angew. Chem.* **2004**, *116*, 6631–6633; *Angew. Chem. Int. Ed.* **2004**, *43*, 6469–6471.
[10] J. Lee, A. O. Govorov, N. A. Kotov, *Angew. Chem.* **2005**, *117*, 7605–7608; *Angew. Chem. Int. Ed.* **2005**, *44*, 7439–7442.
[11] D. Stamou, C. Duschl, E. Delamarche, H. Vogel, *Angew. Chem.* **2003**, *115*, 5580–5583; *Angew. Chem. Int. Ed.* **2003**, *42*, 5738–5741.
[12] P. Hazarika, B. Ceyhan, C. M. Niemeyer, *Small* **2005**, *1*, 844–848.
[13] A. A. M. Thomas, T. R. Vrijsen, A. Boeyé, *J. Virol.* **1986**, *59*, 479–485.
[14] H. P. Taylor, S. J. Armstrong, N. J. Dimmock, *Virology* **1987**, *159*, 288–298.
[15] C. Wohlfart, *J. Virol.* **1988**, *62*, 2321–2328.
[16] J. Icenogle, H. Shiwen, G. Duke, S. Gilbert, R. Rueckert, J. Anderegg, *Virology* **1983**, *127*, 412–425.
[17] H. P. Taylor, N. J. Dimmock, *Virology* **1994**, *205*, 360–363.
[18] T. J. Smith, N. H. Olson, R. H. Cheng, H. Liu, E. S. Chase, W. M. Lee, D. M. Leippe, A. G. Mosser, R. R. Rueckert, T. S. Baker, *J. Virol.* **1993**, *67*, 1148–1158.
[19] A. Flamand, H. Raux, Y. Gaudin, R. W. H. Ruigrok, *Virology* **1993**, *194*, 302–313.
[20] V. M. Okun, R. Moser, D. Blaas, E. Kenndler, *Anal. Chem.* **2001**, *73*, 3900–3906.
[21] A. Azimzadeh, M. H. V. Van Regenmortel, *J. Immunol. Methods* **1991**, *141*, 199–208.
[22] K. Ke, E. F. Hasselbrink, A. J. Hunt, *Anal. Chem.* **2005**, *77*, 5083–5088.
[23] G. K. von Schulthess, G. B. Benedek, R. W. DeBlois, *Macromolecules* **1980**, *13*, 939–945.

[24] G. K. von Schulthess, G. B. Benedek, R. W. DeBlois, *Macromolecules* **1983**, *16*, 434 – 440.
[25] J. J. Kasianowicz, E. Brandin, D. Branton, D. W. Deamer, *Proc. Natl. Acad. Sci. USA* **1996**, *93*, 13770 – 13773.
[26] S. Howorka, S. Cheley, H. Bayley, *Nat. Biotechnol.* **2001**, *19*, 636 – 639.
[27] J. Li, D. Stein, C. McMullan, D. Branton, M. J. Aziz, J. A. Golovchenko, *Nature* **2001**, *412*, 166 – 169.
[28] O. A. Saleh, L. L. Sohn, *Nano Lett.* **2003**, *3*, 37 – 38.
[29] J. Li, M. Gershow, D. Stein, E. Brandin, J. A. Golovchenko, *Nat. Mater.* **2003**, *2*, 611 – 615.
[30] A. F. Sauer-Budge, J. A. Nyamwanda, D. K. Lubensky, D. Branton, *Phys. Rev. Lett.* **2003**, *90*, 238101.
[31] H. Chang, F. Kosari, G. Andreadakis, M. A. Alam, G. Vasmatzis, R. Bashir, *Nano Lett.* **2004**, *4*, 1551 – 1556.
[32] A. Aksimentiev, J. B. Heng, G. Timp, K. Schulten, *Biophys. J.* **2004**, *87*, 2086 – 2097.
[33] A. Mara, Z. Siwy, C. Trautmann, J. Wan, F. Kamme, *Nano Lett.* **2004**, *4*, 497 – 501.
[34] J. B. Heng, C. Ho, T. Kim, R. Timp, A. Aksimentiev, Y. V. Grinkova, S. Sligar, K. Schulten, G. Timp, *Biophys. J.* **2004**, *87*, 2905 – 2911.
[35] P. Chen, J. Gu, E. Brandin, Y. Kim, Q. Wang, D. Branton, *Nano Lett.* **2004**, *4*, 2293 – 2298.
[36] A. J. Storm, J. H. Chen, H. W. Zandbergen, C. Dekker, *Phys. Rev. E* **2005**, *71*, 051903.
[37] E. Berkane, F. Orlik, A. Charbit, C. Danelon, D. Fournier, R. Benz, M. Winterhalter, *J. Nanobiotechnol.* **2005**, *3*, 3.
[38] A. J. Storm, C. Storm, J. Chen, H. Xandbergen, J. Joanny, C. Dekker, *Nano Lett.* **2005**, *5*, 1193 – 1197.
[39] H. Yan, B. Xu, *Small* **2006**, *2*, 310 – 312.
[40] R. M. M. Smeets, U. F. Keyser, D. Krapf, M. Wu, N. H. Dekker, C. Dekker, *Nano Lett.* **2006**, *6*, 89 – 95.
[41] R. W. DeBlois, C. P. Bean, *Rev. Sci. Instrum.* **1970**, *41*, 909 – 916.
[42] R. W. DeBlois, C. P. Bean, R. K. A. Wesley, *J. Colloid Interface Sci.* **1977**, *61*, 323 – 335.
[43] L. Sun, R. M. Crooks, *J. Am. Chem. Soc.* **2000**, *122*, 12340 – 12345.
[44] O. A. Saleh, L. L. Sohn, *Rev. Sci. Instrum.* **2001**, *72*, 4449 – 4451.
[45] T. Ito, L. Sun, R. M. Crooks, *Anal. Chem.* **2003**, *75*, 2399 – 2406.
[46] T. Ito, L. Sun, M. A. Bevan, R. M. Crooks, *Langmuir* **2004**, *20*, 6940 – 6945.
[47] S. Lee, Y. Zhang, H. S. White, C. C. Harrell, C. R. Martin, *Anal. Chem.* **2004**, *76*, 6108 – 6115.
[48] O. A. Saleh, L. L. Sohn, *Proc. Natl. Acad. Sci. USA* **2003**, *100*, 820 – 824.
[49] S. Howorka, J. Nam, H. Bayley, D. Kahne, *Angew. Chem.* **2004**, *116*, 860 – 864; *Angew. Chem. Int. Ed.* **2004**, *43*, 842 – 846.
[50] Z. Siwy, L. Trofin, P. Kohli, L. A. Baker, C. Trautmann, C. R. Martin, *J. Am. Chem. Soc.* **2005**, *127*, 5000 – 5001.
[51] J. D. Uram, K. Ke, A. J. Hunt, M. Mayer, *Angew. Chem.* **2006**, *118*, 2339 – 2343; *Angew. Chem. Int. Ed.* **2006**, *45*, 2281 – 2285.
[52] A. Carbonaro, L. L. Sohn, *Lab on a Chip* **2005**, *5*, 1155 – 1160.
[53] L. Gu, O. Braha, S. Conlan, S. Cheley, H. Bayley, *Nature* **1999**, *398*, 686 – 690.
[54] L. Kullman, M. Winterhalter, S. M. Bezrukov, *Biophys. J.* **2002**, *82*, 803 – 812.
[55] E. A. Heins, Z. S. Siwy, L. A. Baker, C. R. Martin, *Nano Lett.* **2005**, *5*, 1824 – 1829.
[56] R. W. DeBlois, R. K. A. Wesley, *J. Virol.* **1977**, *23*, 227 – 233.
[57] R. W. DeBlois, E. E. Uzgiris, D. H. Cluxton, H. M. Mazzone, *Anal. Biochem.* **1978**, *90*, 273 – 288.
[58] B. I. Feuer, E. E. Uzgiris, R. W. Deblois, D. H. Cluxton, J. Lenard, *Virology* **1978**, *90*, 156 – 161.
[59] C. B. Schaffer, A. Brodeur, J. F. García, E. Mazur, *Opt. Lett.* **2001**, *26*, 93 – 95.
[60] A. P. Joglekar, H. Liu, G. J. Spooner, E. Meyhöfer, G. Mourou, A. J. Hunt, *Appl. Phys. B* **2003**, *77*, 25 – 30.
[61] A. P. Joglekar, H. Liu, E. Meyhöfer, G. Mourou, A. J. Hunt, *Proc. Natl. Acad. Sci. USA* **2004**, *101*, 5856 – 5861.
[62] K. Ke, E. Hasselbrink, A. J. Hunt, *Proc. SPIE-Int. Soc. Opt. Eng.* **2005**, *5714*, 53 – 62.
[63] C. Schmidt, M. Mayer, H. Vogel, *Angew. Chem.* **2000**, *112*, 3267 – 3270; *Angew. Chem. Int. Ed.* **2000**, *39*, 3137 – 3140.
[64] J. L. Rae, R. A. Levis, *Methods Enzymol.* **1992**, *207*, 66 – 92.
[65] M. Mayer, J. K. Kriebel, M. T. Tosteson, G. M. Whitesides, *Biophys. J.* **2003**, *85*, 2684 – 2695.
[66] R. K. Eckhoff, *J. Sci. Instrum.* **1967**, *44*, 648 – 649.
[67] E. W. Weisstein, From MathWorld–A Wolfram Web Resource. http://mathworld.wolfram.com/Icosahedron.html.
[68] W. Chiu, *Annu. Rev. Biophys. Biophys. Chem.* **1986**, *15*, 237 – 257.
[69] T. S. Baker, N. H. Olson, S. D. Fuller, *Microbiol. Mol. Biol. Rev.* **1999**, *63*, 862 – 922.
[70] I. Wang, Y. Li, Q. Que, M. Bhattacharya, L. C. Lane, W. G. Chaney, J. L. Van Etten, *Proc. Natl. Acad. Sci. USA* **1993**, *90*, 3840 – 3844.
[71] S. W. Schneider, J. Lärmer, R. M. Henderson, H. Oberleithner, *Pflügers Arch.* **1998**, *435*, 362 – 367.
[72] N. Nandhagopal, A. A. Simpson, J. R. Gurnon, X. Yan, T. S. Baker, M. V. Graves, J. L. Van Etten, M. G. Rossmann, *Proc. Natl. Acad. Sci. USA* **2002**, *99*, 14758 – 14763.
[73] R. Bashir, *Adv. Drug Delivery Rev.* **2004**, *56*, 1565 – 1586.

Received: January 4, 2006
Revised: March 24, 2006
Published online on June 21, 2006

